Near-Field Synthesis of 1-D Shaped Patterns through Spectral Factorization and Minimally-Redundant Array-Like Representations

Near-Field Synthesis of 1-D Shaped Patterns through Spectral Factorization and Minimally-Redundant Array-Like Representations

Giada M. Battaglia, Tommaso Isernia, Roberta Palmeri, Maria A. Maisto, Raffaele Solimene, and Andrea F. Morabito

***Abstract*—We introduce a novel approach for the mask-constrained power synthesis of 1-D fields enabling near-field shaping according to arbitrary masks. This method presents an innovative framework based on the spectral factorization technique and a warping strategy, allowing for an accurate representation of the near field as a minimally redundant bandlimited function. This provides valuable theoretical tools to effectively solve the problem. In fact, the synthesis is formulated as a linear programming problem followed by a polynomial factorization. Additionally, the approach allows for the a-priori identification of the minimum size of the source required to fulfill a given near-field intensity mask.**

***Index Terms*—Antenna pattern synthesis, array antennas, near-field synthesis, shaped beams, warping sampling.**

I. Introduction

The synthesis of shaped beams represents a canonical problem in antenna theory, with significant applications across several fields such as biomedical engineering [1]-[3], radar systems [4], cellular telecommunications [5], and many more [6]-[32].

Among the different methods addressing this issue, the 'mask-constrained field intensity' synthesis approach stands out as the most effective for achieving the optimal radiation performance [7].

In fact, this formulation acts on the field intensity rather than the complex radiated field, thereby avoiding any a-priori restriction on the field's phase. Furthermore, by constraining the power distribution within a prescribed mask (defined by lower bound and upper bound functions), this approach maximizes the exploitation of the degrees of freedom, providing greater flexibility as compared to pursuing a 'nominal' distribution [7]. Additionally, it allows for complete control over the sidelobe level (SLL).

Despite its potential for superior radiation performance, the 'mask-constrained field intensity' framework is more complex than other formulations. In fact, unlike the 'field synthesis' formulation, it leads to a non-linear relationship between the source and the desired radiation distribution. Moreover, the inclusion of a lower-bound mask requires addressing non-convex constraints [8].

For the far-field case, the Spectral Factorization (SF) method has emerged as a solution to these challenges, offering a mask-constrained field-intensity synthesis approach that guarantees the best possible performance in several relevant cases [33]-[34].

Initially applied to antenna synthesis in 1994 [33] and later to design of finite impulse response filters in 1996 [34], SF has been fully developed for the far-field synthesis of 1-D equispaced arrays, as detailed in the 1998 paper [7] and the 1999 book chapter [35]. This straightforward and deterministic procedure allows for the a-priori determination of whether a prescribed field-intensity mask can be fulfilled by a 1-D source of given size and, if so, identifies all possible source distributions corresponding to the desired field intensity. These capabilities stem from the method's optimal exploitation of the bandlimited nature of the far-field intensity, which allows for the expansion of the field as a trigonometric polynomial. Accordingly, the problem is phrased as the determination of the coefficients of this polynomial, that is cast as a Linear Programming optimization problem followed by a polynomial factorization and a 'zero pairing and flipping' procedure.

SF brings decisive advantages in terms of computational burden and optimality of solution over the state-of-the-art techniques [10]. Furthermore, it is more effective than all the methods that, as the Elliott's one [24], directly act on the roots of the field representation rather than on the coefficients of the field-intensity polynomial.

This is the accepted version of the following article: Giada M. Battaglia, Tommaso Isernia, Roberta Palmeri, Maria A. Maisto, Raffaele Solimene, and Andrea F. Morabito, "Near-Field Synthesis of 1-D Shaped Patterns through Spectral Factorization and Minimally-Redundant Array-Like Representations," IEEE Transactions on Antennas and Propagation, DOI 10.1109/TAP.2024.3525137.

However, SF's application is restricted to cases where the field and its representation comply with the two following specifications:

(1) the field must be (or be possibly conceived as) a 1-D function;

(2) the field has to be represented as a minimally-redundant still accurate trigonometric polynomial. In fact, the requirement for a low-order polynomial is necessary for a robust and effective solution to the subsequent ill-posed inverse source problem (see below).

Requirement (1) is necessary because the Fundamental Theorem of Algebra [36] does not hold true in the 2-D case. For this reason, SF was originally developed only for 1-D equispaced arrays whose far field can be expressed as the array factor. However, the approach has then been extended to several far-field cases, including 1-D arrays subject to mutual-coupling and mounting-platform effects [10], 1-D continuous aperture sources plus sparse isophoric arrays [11], 2-D circularly-symmetric continuous sources [13] (also leading to circular-ring sparse isophoric arrays [37]), and rhombic equispaced 2-D arrays generating circularly-symmetric field intensities [14].

Given the growing interest in near-field communications and sensing [38]-[42], as well as in near-field wireless power transfer [43]-[46], near-field synthesis, i.e., achieving specific electromagnetic field distributions in the near-field region, has triggerered increasing interest in antenna engineering [47]-[49] with many different possible applications (see [47] for a partial list). While many efforts have been devoted to the case of focused fields (with applications in local hyperthermia, wireless power transfer, and many more), applications such as short-range wireless networks and radars, multi-point wireless power transfer, reconfigurable intelligent surfaces [38]-[39], and many more require indeed the consideration of shaped beams.

However, the few existing approaches to the near-field synthesis of shaped patterns either rely on computationally intensive global optimization algorithms (see for instance [9]) or cannot always guarantee the solution's optimality. Consequently, there is a significant lack of methods for the mask-constrained power synthesis that can bring all the SF's advantages to the near-field case. Therefore, the aim here is to introduce a novel approach for the near-field synthesis of shaped patterns having all the SF's advantages. This effort addresses a key limitation, as requirement (2) has historically restricted the application of SF methodologies to far-field scenarios.

In this regard, since the field is a square-integrable function (it is indeed even more regular), it can be approximated by a bandlimited function. In fact, bandlimited functions are dense in the set of finite-energy functions [50]. Accordingly, the representation error can be controlled by carefully choosing a sufficiently large bandwidth. Then, Dirichlet sampling series (and hence a Fourier-like expansions, as the array factor in the far-field zone) can be developed, which would allow to exploit the same procedures as in [7]. This would result in the usual $\lambda/2$ sampling, where λ denotes the wavelength.

On the other hand, such a choice would eventually lead to high-order polynomials, and hence to variations that are not consistent with the actual Number of Degrees of Freedom (NDF) [51] of the field on the measurement line at hand. Consequently, the residual step from field representation to the actual source would be either inaccurate or unstable, rendering the solution non-effective.

In order to restore consistency amongst the actual NDF and the order of a polynomial representation, in the following we leverage convenient near-field representation strategies [52]-[54]. These latter are based on the so-called 'reduced radiated field' concept and on a proper recasting of the radiation operator by certain warping transformations. In fact, with proper parametrization, the degrees of freedom of the field on a truncated observation domain correspond to the number of samples of the 'reduced field' on that domain, provided samples are properly collected [52],[55],[56].

Notably, in such a way, the corresponding trigonometric polynomial approximation is of finite order even for unbounded domains. This agrees with the finiteness of the NDF of the near-field (when evanescent waves are negligible), regardless of the size of the observation domain [57].

The proposed approach addresses the 1-D near-field power synthesis by generating shaped beams lying within an arbitrary mask defined in the warped domain. Accordingly, for the first time in the literature, the near-field mask-constrained power synthesis problem is definitively solved by using the SF technique, retaining all its advantages.

The main features of the developed procedure have been briefly described in the conference contribution [58]. This latter has been aimed only to provide a brief overview of the proposed approach and, hence, it does not include either the full technical development of the method or the numerical experiments presented in this paper.

In the following, the details of the devised synthesis approach are reported by Section II, while numerical examples are shown in Section III. Conclusions follow.

II. The Proposed Approach

To convey the idea, we consider a linear radiating structure supported over the 'source domain' $SD = [-a, a]$ along the x-axis. The current can be continuously distributed, representing an antenna aperture supported over SD, or discrete as for array antennas.

This is the accepted version of the following article: Giada M. Battaglia, Tommaso Isernia, Roberta Palmeri, Maria A. Maisto, Raffaele Solimene, and Andrea F. Morabito, "Near-Field Synthesis of 1-D Shaped Patterns through Spectral Factorization and Minimally-Redundant Array-Like Representations," IEEE Transactions on Antennas and Propagation, DOI 10.1109/TAP.2024.3525137.

The goal is to synthesize a field with a desired field intensity over the 'observation domain' $OD = [-X_o, X_o]$, spanned by the variable x_o, parallel to SD and located in the near-field region of the source at a distance $z = z_o$. Here, we specifically focus on OD located in the radiative near-field, where radiation effects dominate over reactive components, making this region particularly relevant for practical antenna synthesis. By concentrating on this region, we avoid the complexities and potential instability introduced by reactive fields. Furthermore, we limit our analysis to non-superdirective sources whose minimum extension exceeds some wavelengths. This allows us to apply established results on the degrees of freedom of the radiated field and non-redundant field representations [53], [54].

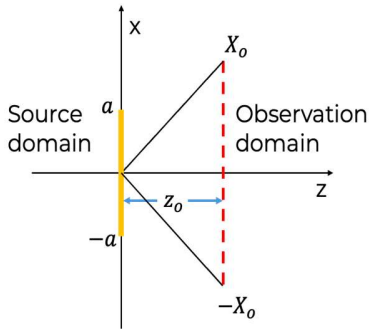

Fig. 1. Geometry of the problem (from [53]).

We assume that the current is linearly polarized and directed along the y-axis. Consequently, the synthesis problem concerns the shaping of the y-component of the field. See Fig. 1 for a pictorial description of the geometry of the problem.

To proceed, as mentioned in the previous Section, it proves convenient to find a proper polynomial representation for the near field. As argued there, a bandlimited function can always be identified for this purpose, and the key lies in an optimal choice of its representation.

The desired near-field representation can be conveniently obtained by exploiting the analytical properties of the radiated field. According to [53], which aligns with the theory in [52] for 1-D sources, the range of the radiation operator for non-superdirective sources of bounded support can be approximated as the set of spatially varying bandlimited functions, with the band depending only on the source size and the distance from OD. Specifically, when the field is regarded as a function of the so-called 'warping variable' $\zeta(x_o)$, i.e.:

$$\zeta(x_o) = \frac{\beta}{2}\left[\sqrt{(x_o + a)^2 + z_0^2} - \sqrt{(x_o - a)^2 + z_0^2}\right] \quad (1)$$

(where β is the wavenumber and x_o the original observation variable), it can be approximated as the product of an exponential phase term times a bandlimited function having bandwidth $\Omega_\zeta = [-1,1]$, i.e.:

$$E[\zeta(x_o)] = e^{-j\gamma(x_o)} \int_{-1}^{1} \hat{E}(w) e^{-jw\zeta(x_o)} dw \quad (2)$$

where $\hat{E}(w)$ denotes the spectrum, and

$$\gamma(x_o) = \frac{\beta}{2}\left[\sqrt{(x_o + a)^2 + z_0^2} + \sqrt{(x_o - a)^2 + z_0^2}\right] \quad (3)$$

Basically, the transformation (1) stretches $OD = [-X_o, X_o]$ into $OD_\zeta = [\zeta(-X_o), \zeta(X_o)]$, which remains finite even when OD is unbounded, resulting in the aforementioned bandlimited approximation. Note that the bandwidth value is immaterial and results from the particular choice of the scaling factor in (1). A different choice would lead to a scaled Ω_ζ, with ζ ranging over an interval of different size. However, the product $m[OD_\zeta]m[\Omega_\zeta]$, with $m[\cdot]$ representing the measure, always remains constant (refer to [54] for more details).

By exploiting the warping representation (2) and invoking the concentration properties of prolate spheroidal wavefunctions, which effectively approximate the singular functions of the radiation operator relating the source to the field on the domain at hand [59], it can be concluded that the field belongs to a finite-dimensional space. The dimension of this space is $M = \frac{2\zeta(X_o)}{\pi}$ and corresponds to the NDF for the considered near-field configuration [54]. This entitles us to look for a more convenient finite-dimensional representation of the field in terms of bandlimited trigonometric polynomials, approximating the Fourier integral as a finite Riemann sum [56] (see also [53],[54]). Consequently, the following finite-dimensional representation of the field can be achieved:

$$E(\tilde{x}) = e^{-j\,(x_o)} \sum_{n=-\frac{M}{2}}^{\frac{M}{2}} c_n e^{jn\tilde{x}} \quad (4)$$

with

$$-\pi \le \tilde{x} = \frac{\pi\zeta(x_o)}{\zeta(X_o)} \le \pi \quad (5)$$

It is important to note that since relation (1) is injective, the interval $[-X_o, X_o]$ is univocally mapped into the interval $[-\tilde{x}(X_o), \tilde{x}(X_o)]$. Therefore, any mask required to shape the field amplitude in the 'real' domain $[-X_o, X_o]$ can be equivalently applied in the 'warped' domain $[\tilde{x}(-X_o), \tilde{x}(X_o)]$ and vice versa.

It is remarked that the warping variable plays a crucial role in our approach. Firstly, it allows to regain Fourier-based

This is the accepted version of the following article: Giada M. Battaglia, Tommaso Isernia, Roberta Palmeri, Maria A. Maisto, Raffaele Solimene, and Andrea F. Morabito, "Near-Field Synthesis of 1-D Shaped Patterns through Spectral Factorization and Minimally-Redundant Array-Like Representations," IEEE Transactions on Antennas and Propagation, DOI 10.1109/TAP.2024.3525137.

arguments and hence to come to the field representation/approximation (4) in terms of a trigonometric polynomial. Secondly, and more importantly, the warping formalism provides a highly efficient and non-redundant representation of the range of the radiation operator [53], which in turn ensures a minimal-order representation. This offers two decisive advantages:

- while any trigonometric-like representation (even in the original variable) can permit SF of the square amplitude field, it can result in excessively high order polynomials, thus complicating the factorization process;
- the resulting field is already projected on the so-called 'essential' range of the radiation operator, i.e., the one spanned by the singular functions corresponding to the most relevant singular values of the radiation operator [54]. Accordingly, the warping implicitly helps in regularizing the inverse source problem and thus in avoiding rapidly oscillating sources as well as sources characterized by a large dynamic range, which would be difficult or even impossible to be realized in practice.

Consequently, apart from superdirective sources, the field radiated by any source within the interval [$-a$,a] can be effectively represented by using the warping formalism [53],[60] and equation (4). What is more, since the warping reflects the mathematical properties of the radiation operator (and not of the particular source), it works regardless the source is continuous or discrete.

Turning to (4), apart from the exponential term in front of the summation, it resembles an array factor. In fact, one can write:

$$E(\tilde{x}) = e^{-j\gamma(x_o)}F(\tilde{x}) \tag{6}$$

where

$$F(\tilde{x}) = \sum_{n=-\frac{M}{2}}^{\frac{M}{2}} c_n e^{jn\tilde{x}} \tag{7}$$

As a result, this approach enables the development and exploitation of the SF method [7] for the near-field case through the following three-step procedure.

Step 1. Identification of the optimal near-field intensity

By recognizing that the first factor in front of (6) disappears when calculating the square amplitude, and following the arguments in [7], the square amplitude of (6) can be written as:

$$P(\tilde{x}) = \sum_{p=-M}^{M} D_p e^{jp\tilde{x}} \tag{8}$$

where $P(\tilde{x})$ must be a real function, implying that the coefficients D_p (with $p = -M, \dots, M$) form a Hermitian sequence.

Then, a *feasibility criterion* is applied to conceive $P(\tilde{x})$ as a function that satisfies a desired power mask, defined by an upper bound (UB) function and a lower bound (LB) function. Thanks to (1), constraints in the original spatial variable are translated into constraints in terms of $\tilde{x}$. The field intensity is then identified by solving the following Linear Programming (LP) optimization problem:

Find $D_{-M}, \dots, D_{-1}, D_0, D_1, \dots, D_M$ *in such a way that:*

$$LB(\tilde{x}) \leq \sum_{p=-M}^{M} D_p e^{jp\tilde{x}} \leq UB(\tilde{x}) \tag{9.a}$$

$$D_p = D_{-p}^* \quad for\ p = 1, \dots, M \tag{9.b}$$

where * denotes complex conjugation.

Notably, as in the far-field case discussed in [7] and [33], finding a solution to (9) is not only a *necessary* condition for the existence of the desired field intensity but, by virtue of the Fejer-Riesz theorem [61], it is also a *sufficient* condition for the existence of a function of the kind (6) to represent the near field. Hence, (9) represents an *existence criterion* as well.

Notably, this step of the procedure also enables the identification of the minimal source size for a given performance or, in a dual fashion, allows for maximizing performance for a given source size. In fact, the computational efficiency of the LP step allows for the a-priori (i.e., before performing the actual synthesis) identification of the minimum source size required for the feasibility of the given mask, thus transforming the 'synthesis' into an 'optimal synthesis' [13]. This is achieved by iteratively solving (9) with progressively smaller values of a until the constraints become too stringent to allow for any solution.

It is worth noting that formulation (9) also allows adding the minimization of an objective function aimed at maximizing some field-intensity related performance, e.g., beam efficiency or directivity.

Step 2. Application of the SF technique

Once $P(\tilde{x})$ has been determined, the SF technique is applied to identify the corresponding complex field factor $F(\tilde{x})$ such that $|F(\tilde{x})|^2 = P(\tilde{x})$.

This process involves determining the roots of $P(\tilde{x})$ and then applying the Fejér-Riesz theorem [61] to factorize the underlying polynomial as:

$$P(\tilde{x}) = F(\tilde{x})F^*(\tilde{x}) \tag{10}$$

Since $P(\tilde{x})$ is a real and non-negative trigonometric polynomial, if $\tilde{z}$ is one of its zeroes, then $\frac{1}{\tilde{z}^*}$ is a zero as well,

This is the accepted version of the following article: Giada M. Battaglia, Tommaso Isernia, Roberta Palmeri, Maria A. Maisto, Raffaele Solimene, and Andrea F. Morabito, "Near-Field Synthesis of 1-D Shaped Patterns through Spectral Factorization and Minimally-Redundant Array-Like Representations," IEEE Transactions on Antennas and Propagation, DOI 10.1109/TAP.2024.3525137.

and the roots on the unit circle always appear in pairs. This entails that the factorization (10) is not unique, as a zero-flipping procedure can be used to find different $F(\tilde{x})$ distributions all corresponding to the same field intensity. By virtue of such a circumstance, the proposed approach will return not one but all the different sources that can radiate the desired field intensity. This flexibility is particularly useful, as it allows also the selection of the most easily realizable source. In fact, the availability of multiple solutions enables the user to choose the most suitable one based on specific practical criteria, such as the source with the lowest dynamic range ratio, the one that can be most easily discretized into a sparse array, or the one that facilitates reconfiguration of the field to different radiation modalities [11].

Step 3. Determination of the source

Once an $F(\tilde{x})$ distribution fulfilling (10) has been determined, the next step is to identify the source that radiates this field.

To this end, the phase term in front of the summation in equation (4), which is lost when transitioning from (4) to the field intensity in (8), must first be restored. This yields the actual radiated field as $E(x_o) = F[\tilde{x}(x_o)]e^{-j\gamma(x_o)}$. Then, the source is identified by solving an inverse source problem as described below. In particular, in the following we separately address the cases of continuous and discrete currents.

Step 3/case I: Synthesis of continuous sources

We start by considering the case of continuous current distributions (subject to non-super-directivity constraints) since they allow for an early assessment of the performance limits of any aperture antenna of a given size, even before choosing the specific radiating elements or technology. Indeed, repeated application of the initial feasibility step allows for identifying the minimal dimensions of the radiating system that are required to achieve a given performance or, conversely, for maximizing performance within given dimensions. In fact, their (source and pattern) distributions can act as a reference, target, and benchmark for practical implementations [11],[37].

In this case, the relationship between the radiated field and the source is given by the following radiation operator:

$$E(x_o) = \int_{-a}^{a} G(x_o, x; \beta) J(x) dx \tag{11}$$

where J represents the continuous electric or magnetic current and $G(x_o, x; \beta) = \frac{e^{-j\beta|\boldsymbol{r}-\boldsymbol{r_0}|}}{|\boldsymbol{r}-\boldsymbol{r_0}|}$ is the 3-D Green function, up to some unessential scalar factors, with $|\boldsymbol{r}-\boldsymbol{r_0}| = \sqrt{(x_o - x)^2 + z_o^2}$. This compact operator can be discretized by exploiting a sufficiently dense grid of points on both the source and observation domains. The source J is then determined by using a Truncated Singular Value Decomposition (TSVD) regularizing inversion scheme, i.e.:

$$J = \sum_{n=0}^{M} \frac{< E, v_n >}{\sigma_n} u_n \tag{12}$$

where u_n, σ_n, v_n are the singular system of the discretized radiation operator, and the TSVD expansion is truncated at the nominal NDF, i.e., M.

As already stated, the adopted near-field representation does not include fields corresponding to superdirective sources, thus ensuring that one (or more) 'smooth' source distributions can be safely obtained with a negligible field misfit.

Before leaving this Section, it is worth pausing a little bit on the inversion formula (12). Since a synthesis problem is being addressed (and not a retrieval problem where data are always corrupted by noise), one might question the need for regularization and the specific truncation at the NDF.

Indeed, solving (12) involves the inversion of a compact operator with a step-like singular values distribution [54] and wherein (see [62],[63]) the singular functions v_n exhibit similar concentration properties as the prolate spheroidal wavefunctions [64]. As a consequence, choosing M larger than the NDF would result in sources which would affect the field values outside the linear interval of interest. In fact, the first M singular functions are primarily concentrated (in energy) within $[-X_o, X_o]$, while the remaining functions are more relevant outside OD. Thus, retaining more than M singular functions in (12) would cause the radiated field to increase outside $[-X_o, X_o]$, as shown in one of the numerical examples reported in the next numerical Section.

Step 3/case II: Synthesis of actual discrete sources

As a last (but not least) point, one has to consider the possibility of achieving a power pattern that satisfies the desired power mask through an actual antenna, and we focus herein on the case of an array. Hence, after obtaining an $F(\tilde{x})$ distribution that meets the criteria in (10), the next step is to identify a discrete source J that can radiate this field.

In this regard, it is well-known that the far-field radiated by any non-superdirective continuous source can be realized by an equispaced array antenna with an inter-element spacing equal to or slightly lower than $\frac{\lambda}{2}$ without altering the radiated field [11],[65]-[67].

In the radiative near-field zone considered herein, the following theoretical arguments, and the example provided in the next Section, indicate that accurate realization of the given field through discrete sources is still viable.

Indeed, as the adopted near-field representation does not allow for superdirective components, the equivalence amongst

This is the accepted version of the following article: Giada M. Battaglia, Tommaso Isernia, Roberta Palmeri, Maria A. Maisto, Raffaele Solimene, and Andrea F. Morabito, "Near-Field Synthesis of 1-D Shaped Patterns through Spectral Factorization and Minimally-Redundant Array-Like Representations," IEEE Transactions on Antennas and Propagation, DOI 10.1109/TAP.2024.3525137.

discrete and continuous sources observed in the far-field also applies to the radiative near-field. In fact, for non-superdirective sources, far-field equivalence implies spectral equivalence, and thus radiative field equivalence, as long as the observation line is outside the reactive zone. Consequently, only very small deviations in the realized fields are expected (as also shown by the numerical experiments presented in Section III).

Moving on, once a technology has been selected, the problem consists in determining the array excitations. To this end, different strategies can be employed, some of which can directly exploit the continuous sources obtainable as discussed in the previous subsection.

The first and simplest way to identify the array excitations is that of sampling the continuous current distributions, which is known to be effective in the corresponding far-field case [65]-[67] and, according to previous arguments, still works for the considered near-field configuration.

A second possible strategy, which can be pursued by means of 'density taper' [11],[37],[67] techniques, is to exploit the continuous (real or even complex) source distributions in order to identify the array elements' locations (rather than excitation amplitudes) and hence to design the so-called 'isophoric' (constant-excitation-amplitude) arrays.

A third and last possibility, once the array geometry has been fixed, consists in directly finding the array elements' excitations $I_{-N}, \dots, I_N$ by solving the inverse source problem in a discrete setting.

The third strategy is indeed the one we adopt as it provides a decisive advantage with respect to the other two methods, i.e., it allows to take into account, in a straightforward fashion, the actual radiation pattern of realistic elements including mutual coupling and mounting platform effects. Coming to details, by using an array of $2N+1$ elements directed along the y-axis and located with spacing equal to or slightly lower than $\lambda/2$, eq. (11) becomes:

$$E(x_o) = \sum_{n=-N}^{N} G_n I_n \qquad (13)$$

where $G_n = \frac{e^{-j\beta|\boldsymbol{r_n}-\boldsymbol{r_0}|}}{|\boldsymbol{r_n}-\boldsymbol{r_0}|} f_n(\theta_n, \varphi_n)$, θ_n and φ_n respectively denote the elevation and azimuth angles between $\boldsymbol{r_0} = (x_o, z_o)$ (i.e., the field observation point) and $\boldsymbol{r_n} = (x_n, 0)$ (i.e., the n-th element location), and f_n represents the n-th active element pattern [10] accounting for all the realistic effects affecting the actual radiation behavior of the different array elements (including mutual coupling).

III. Numerical Examples

This Section presents numerical examples to evaluate the effectiveness of the proposed approach for both continuous and discrete sources.

In each test case, once the mask has been set in order to shape the field intensity as desired, the parameter a has been identified by repeatedly solving (9) with progressively smaller source sizes until no solution is found, thereby determining the minimum size of the source required to fulfill the given requirements. Therefore, the maximum theoretical performance achievable by any source of fixed size has been identified for each considered power mask. Additionally, X_0 and z_0 are such to always ensure that the OD is located within the radiative near-field region of the source.

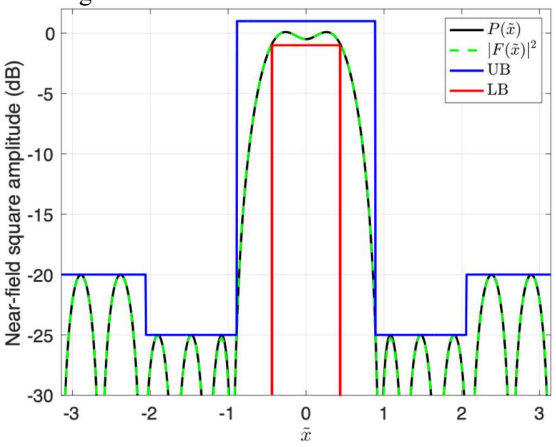

Fig. 2. Synthesis of a flat-top near field: enforced UB (blue curve) and LB (red curve) constraints; near-field intensities achieved after step 1 (black curve) and step 2 (green dashed curve) of the synthesis procedure.

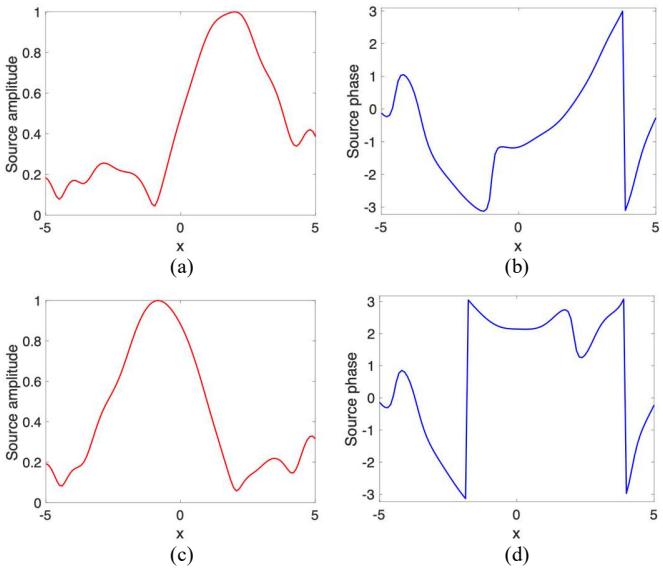

This is the accepted version of the following article: Giada M. Battaglia, Tommaso Isernia, Roberta Palmeri, Maria A. Maisto, Raffaele Solimene, and Andrea F. Morabito, "Near-Field Synthesis of 1-D Shaped Patterns through Spectral Factorization and Minimally-Redundant Array-Like Representations," IEEE Transactions on Antennas and Propagation, DOI 10.1109/TAP.2024.3525137.

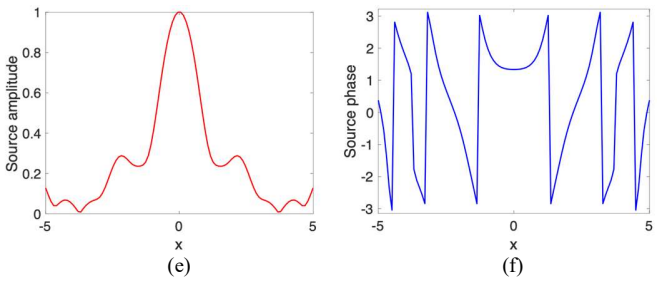

(e) (f)

Fig. 3. Amplitude (on the left) and phase (on the right) of three different sources all radiating the same near-field power pattern plotted in green in Fig. 2.

III.A. Numerical experiments for the synthesis of continuous sources

In the first test case, we set $a = 5\lambda$, $X_0 = 10\lambda$, and $z_0 = 10\lambda$. Furthermore, *UB* and *LB* have been set to generate a near-field flat-top pattern with a ripple equal to $\pm 1\ dB$ and non-uniform sidelobe levels. In particular, as shown in Fig. 2, *UB* has been set as -20 dB for $|\tilde{x}| \geq 2.06$, -25 dB for $0.89 \leq |\tilde{x}| < 2.06$, and 1 dB elsewhere, while *LB* has been set as -1 dB for $|\tilde{x}| \leq 0.45$.

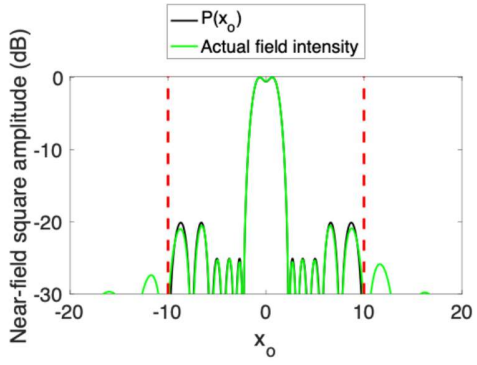

(a)

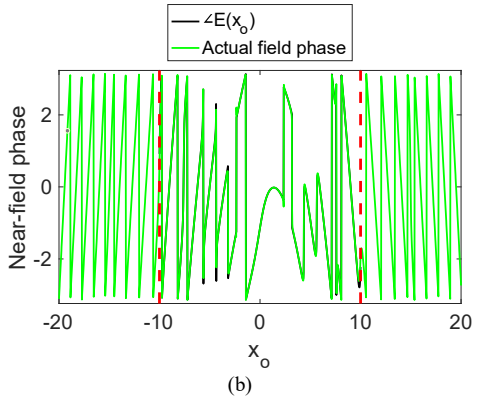

(b)

Fig. 4. Comparison between the field generated by the source shown in Fig. 3(a)-(b) and the field coming out from step 2 of the procedure: (a) square amplitude; (b) phase. The vertical red dashed lines denote OD borders.

The field intensity coming out from step 1 of the synthesis procedure (corresponding to the maximum theoretical performance achievable for the adopted mask and size of the source) is shown in Fig. 2, along with the *UB* and *LB* functions. Then, step 2 allowed to quickly identify the complex fields fulfilling (10), whose square amplitude is superimposed on Fig. 2, matching the field intensity coming out from the solution of (9). As can be seen, the enforced mask is perfectly fulfilled. Finally, step 3 provided a multiplicity of sources radiating the sought power pattern, three of which are shown in Fig. 3.

To verify the reliability of the overall procedure, we compared in Fig. 4 the complex field obtained from step 2 (plus phase restoration) with the field resulting from applying (11) to the synthesized J distribution for one of the sources shown in Fig. 3. As can be seen, both the amplitude and phase align within the masked domain $[-X_o, X_o]$, confirming the effectiveness and accuracy of the approach in pursuing the maximum possible radiation performance. It is also worth noting that, while Fig. 2 shows the field intensity in the warped domain, Fig. 4 depicts the field as a function of the actual spatial variable x_o as extended beyond the borders of the OD (indicated by the vertical red dashed lines). As expected, due to the optimal truncation (at the nominal NDF) of the TSVD expansion, the actual intensity of the radiated field does not rise outside the masked domain $[-X_o, X_o]$.

In the second test case, we address the synthesis of a multifocus near-field pattern, relevant for applications such as multi target wireless power transfer or multi-user near-field communication channels [22]. To this end, we set $a = 7\lambda$, $X_0 = 14\lambda$, and $z_0 = 14\lambda$. Moreover, *UB* and *LB* are set to ensure a ripple of $\pm 1\ dB$ in the shaped-beam zone and a sidelobe level lower than -20 dB elsewhere. Specifically, *UB* is set as -20 dB for $|\tilde{x}| \geq 2$ and $|\tilde{x}| \leq 1.10$, and 1 dB elsewhere. *LB* is set as -1 dB for $1.36 \leq |\tilde{x}| \leq 1.66$.

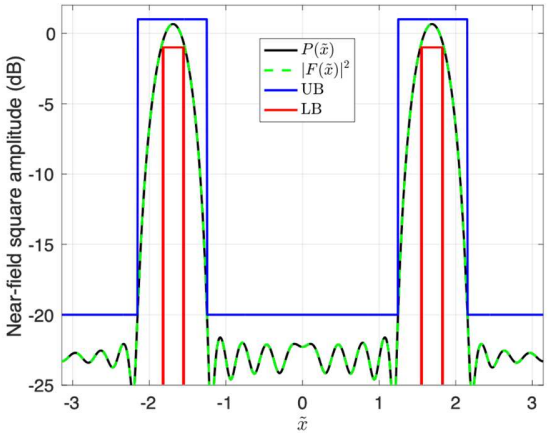

Fig. 5. Synthesis of a multifocused near field: enforced UB (blue curve) and LB (red curve) constraints; near-field intensities coming out from step 1 (black curve) and step 2 (green dashed curve) of the synthesis procedure.

This is the accepted version of the following article: Giada M. Battaglia, Tommaso Isernia, Roberta Palmeri, Maria A. Maisto, Raffaele Solimene, and Andrea F. Morabito, "Near-Field Synthesis of 1-D Shaped Patterns through Spectral Factorization and Minimally-Redundant Array-Like Representations," IEEE Transactions on Antennas and Propagation, DOI 10.1109/TAP.2024.3525137.

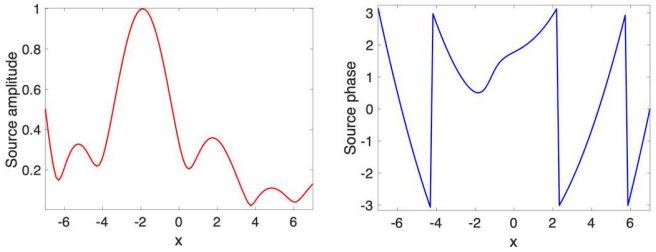

(a) (b)

Fig. 6. Synthesized source radiating the near-field pattern plotted in green in Fig. 5: (a) normalized amplitude; (b) phase.

The adopted mask and the field intensity $P(\tilde{x})$ determined by solving the optimization problem (9) (corresponding to the maximum theoretical performance) are depicted in Fig. 5, while one of the sources identified at the end of the procedure is shown in Fig. 6. It is important to note that, given the electrical source dimensions and that the presentation of phase distributions in a wrapped (rather than unwrapped) form, the source distributions shown in Figures (3) and (6) can be considered to be 'smooth', which agrees with the theoretical characteristics of the warping strategy and allows emulating the corresponding radiative near field by means of a discrete source.

As in the previous test case, to further verify the approach, the field intensity radiated by the synthesized source is superimposed to $P(\tilde{x})$ in Fig. 7, showing that the solution perfectly complies with all specifications, thus confirming the effectiveness of the approach in providing a radiation performance equivalent to the maximum possible one. Notably, Fig. 7 also shows that, although constraints are enforced within $[-X_o, X_o]$, the synthesized field intensity does not rise outside this interval.

In order to show the impact of using an M value larger than the NDF in (12), the numerical example has been repeated by retaining 24 singular functions (while $NDF = 20$ in this case). The results, shown in Fig. 8, demonstrate that the radiated field outside $[-X_o, X_o]$ rises and surpasses the sidelobe mask. This occurs because the exponential base functions employed in the field representation (4) are not exactly equal (in terms of the subspace they span) to the actual singular functions of the radiation operator. As a result, the obtained field projects closely but not exactly onto the subset of the range of the radiation operators spanned by the first M singular functions. This effect is similar to what happens with superdirective currents, where the visible domain in the far-field region is analogous to the near-field OD where constrains are enforced.

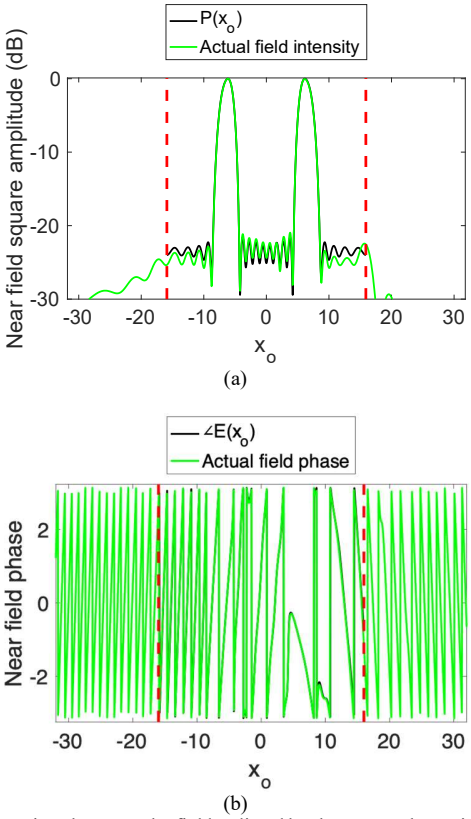

Fig. 7. Comparison between the field radiated by the source shown in Fig. 6 and the field coming out from step 2 of the procedure: (a) square amplitude; (b) phase. The vertical red dashed lines denote OD borders.

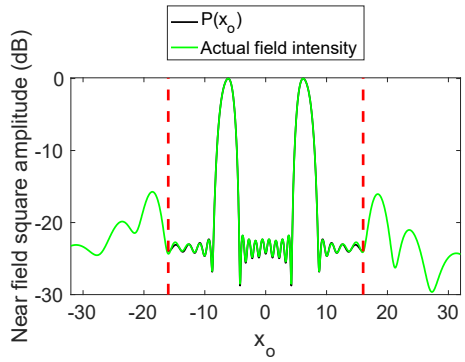

Fig. 8. Synthesis of a multifocused near field: field intensity coming out from step 1 of the synthesis procedure (black curve); field intensity generated by the synthesized source (green curve) when the TSVD truncation index exceeds the NDF. The vertical red dashed lines denote OD borders.

III.B. Numerical experiments for the synthesis of realistic array antennas

This subsection demonstrates the effectiveness of the proposed approach when applied to discrete sources. In particular, the results of the design of the same realistic array as

This is the accepted version of the following article: Giada M. Battaglia, Tommaso Isernia, Roberta Palmeri, Maria A. Maisto, Raffaele Solimene, and Andrea F. Morabito, "Near-Field Synthesis of 1-D Shaped Patterns through Spectral Factorization and Minimally-Redundant Array-Like Representations," IEEE Transactions on Antennas and Propagation, DOI 10.1109/TAP.2024.3525137.

in [21] are compared to both theoretical expectations as well as to the outcomes of [21].

To this end, the considered array configuration and OD are identical to those in [21], i.e., a 1-D linear array with a uniform element distribution consisting of 31 y-oriented dipoles, as shown in Fig. 9, with an element spacing of 0.5λ and an observation area defined as a 15λ-length linear segment along the x-axis.

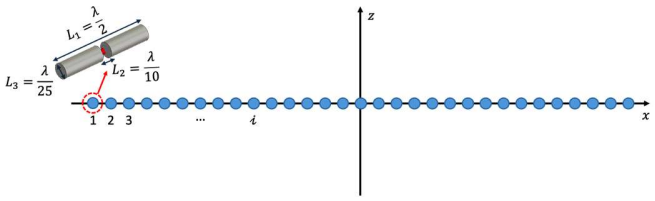

Fig. 9. Structure of the full-wave simulated array.

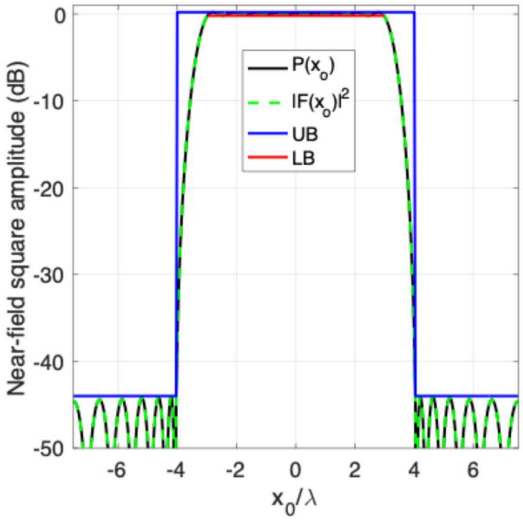

Fig. 10. Synthesis of a flat-top near field (comparison with [21]): enforced UB (blue curve) and LB (red curve); near fields coming out from the feasibility criterion (black curve) and step 2 (green dashed curve) of the synthesis procedure.

In the initial step, following [21] we set the key parameters as $a = 7.5\lambda$, $X_0 = 7.5\lambda$, and $z_0 = 5\lambda$, locating the observation plane within the radiative near-field region of the source. UB and LB values were defined to ensure a ripple of $\pm 0.2dB$ in the shaped zone and a sidelobe level lower than $-44dB$ elsewhere, with UB set to -44 dB for $\left|\frac{x_o}{\lambda}\right| \geq 4$.

The mask and power pattern P were determined by solving the LP problem $LB(\tilde{x}) \leq P(\tilde{x}) \leq UB(\tilde{x})$. The resulting power pattern is shown in Fig. 10, while Fig. 11 provides three of the multiple synthesized excitations that radiate the desired power pattern. Note that the latter are determined by using in (13) the active element patterns computed through full-wave electromagnetic simulations performed by the CST microwave studio, so that mutual coupling effects are also taken into account.

To validate the approach, Fig. 12 compares the complex field coming out from step 2 (including phase restoration) with the full-wave simulated field radiated by one of the synthesized array excitations shown in Fig. 11. The figure and the values summarized in Table I confirm that the final solution is very close to the theoretical limits determined in the second step, and that the method outperforms the one in [21]. These can both be attributed to the initially chosen 'mask constrained' formulation (which does not enforce any restriction on the phase of the field component at hand) as well as to the adopted solution strategy. Also, note that in [21] the CVX-based method uses isotropic elements, while the DRO-based technique employs ideal dipoles (dyadic Green's function) as array elements. In contrast, our example leverages a full-wave electromagnetic simulation to identify the active element pattern associated to each dipole, allowing us to account for potential heterogeneity amongst the radiating elements as well as mutual coupling.

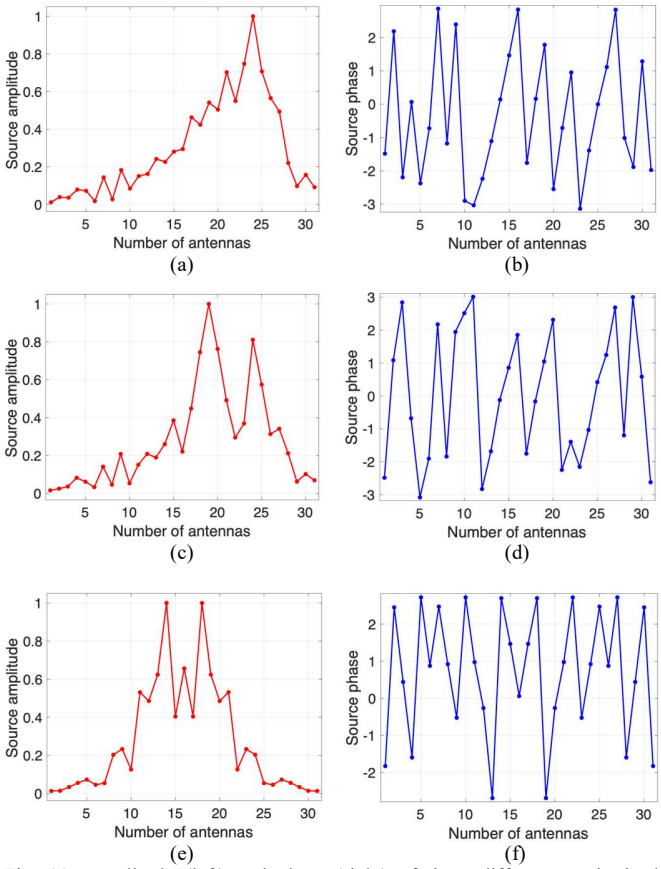

Fig. 11. Amplitude (left) and phase (right) of three different synthesized excitations both radiating the same (sought after) near-field power pattern.

This is the accepted version of the following article: Giada M. Battaglia, Tommaso Isernia, Roberta Palmeri, Maria A. Maisto, Raffaele Solimene, and Andrea F. Morabito, "Near-Field Synthesis of 1-D Shaped Patterns through Spectral Factorization and Minimally-Redundant Array-Like Representations," IEEE Transactions on Antennas and Propagation, DOI 10.1109/TAP.2024.3525137.

	Isotropic elements		Realistic elements	
	CVX [21]	This method	DRO [21]	This method
Ripple [dB]	±0.19	±0.19	±0.13	±0.19
Maximum SLL[dB]	-43	-44	-31	-41

Table I. Radiation performance achieved by the proposed method (comparison with the technique in [21]).

Furthermore, in comparison to [21], a distinctive feature of our method is its generality with respect to the kind of pattern one is looking for. In contrast, the approach in [21] is tailored for flat-top patterns and would require specific reformulations for the many other cases of possible interest, such as cosecant and multifocused patterns as well as fields with non-uniform sidelobes. Finally, our approach has two further considerable advantages. First, it has the capability of identifying a multiplicity of solutions. Second, it includes a built-in feasibility criterion, enabling in advance the determination of whether a given pattern is achievable based solely on the source size, whereas no such criterion is mentioned in [21].

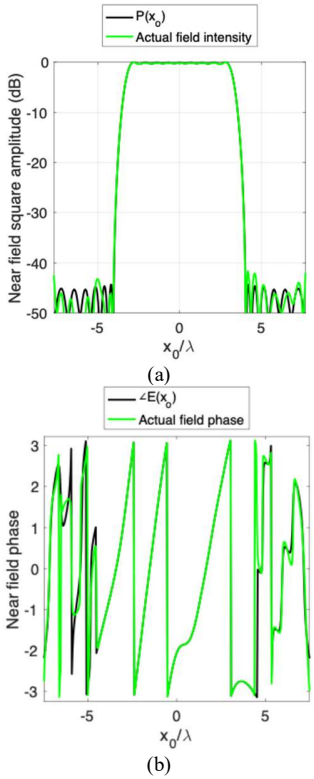

Fig. 12. Superposition between the field radiated by the actual realistic array (as computed by a full-wave simulation with one of the excitation sets shown in Figure 11) (green curve) and the field coming out from spectral factorization (black curve): square amplitude [subplot (a)]; phase [subplot (b)].

IV. Conclusions

Following the increasing interest in near-field communications and sensing [38]-[42], as well as in near-field wireless power transfer [43]-[46], the near-field synthesis of shaped patterns has been dealt with.

In particular, a new and effective procedure has been devised for the optimal synthesis of shaped beams fulfilling an arbitrary power mask in the near-field region.

The developed approach takes maximum advantage of two powerful tools, i.e., the well-established spectral factorization method and a recently-developed warping sampling technique. In fact, while the spectral factorization method has been proven effective for far-field synthesis, its application to near-field scenarios poses challenges due to the complicated nature of the near field. To overcome this limitation, we leveraged warping sampling schemes to represent the near field by means of an 'array-like' representation, facilitating the use of the spectral factorization technique and its remarkable advantages in the near-field scenarios.

Several key advantages distinguish our approach as detailed in the following.

The proposed method is the first one capable of casting the synthesis of shaped beams fulfilling arbitrary masks in the near-field region (using linear sources with limited support) as a linear programming optimization followed by polynomial factorization. Such a circumstance also allows to quickly find all the different sources corresponding to the sought field-intensity distribution, allowing for the selection of the most convenient source for practical implementation.

The method also avoids computationally intensive, 'black box' global optimization procedures, offering a deterministic, non-iterative solution. Furthermore, unlike traditional nominal-field synthesis approaches, which unnecessarily over constrain the results and yield a single, often less effective solution, our technique addresses a mask-constrained power-pattern synthesis problem, allowing for greater flexibility.

Another key advantage of the proposed method is its adaptability to both continuous and discrete sources, as demonstrated by representative examples (including full-wave simulated realistic antennas) that highlight its effectiveness in both cases.

Finally, the thorough characterization of the mathematical properties of the near-field radiation operator offered by the warping sampling theory allows performing the field intensity synthesis over bounded observation domains without incurring in fields growing outside the synthesis domain.

The proposed procedure can be directly used to perform the near-field synthesis of 2-D patterns that are $x-y$ factorable or circularly symmetric. It can also be extended to 2-D fields

This is the accepted version of the following article: Giada M. Battaglia, Tommaso Isernia, Roberta Palmeri, Maria A. Maisto, Raffaele Solimene, and Andrea F. Morabito, "Near-Field Synthesis of 1-D Shaped Patterns through Spectral Factorization and Minimally-Redundant Array-Like Representations," IEEE Transactions on Antennas and Propagation, DOI 10.1109/TAP.2024.3525137.

having arbitrary footprints by using the same philosophy as the one introduced in [68],[69].

REFERENCES

[1] G. Buonanno and S. Costanzo, "Fresnel-Zone Focused Antenna Arrays: Tolerance Analysis for Biomedical Applications," *IEEE Transactions on Antennas and Propagation*, vol. 71, no. 9, pp. 7261-7272, 2023, DOI: 10.1109/TAP.2023.3295493.

[2] M. Alibakhshikenari, B. S. Virdee, P. Shukla, N. O. Parchin, L. Azpilicueta, C. H. See, R. A. Abd-Alhameed, F. Falcone, I. Huynen, T. A. Denidni, and E. Limiti, "Metamaterial-Inspired Antenna Array for Application in Microwave Breast Imaging Systems for Tumor Detection," *IEEE Access*, vol. 8, pp. 174667-174678, 2020, DOI: 10.1109/ACCESS.2020.3025672.

[3] X. Lin, Y. Chen, Z. Gong, B. C. Seet, L. Huang, and Y. Lu, "Ultrawideband Textile Antenna for Wearable Microwave Medical Imaging Applications," *IEEE Transactions on Antennas and Propagation*, vol. 68, no. 6, pp. 4238-4249, 2020, DOI: 10.1109/TAP.2020.2970072.

[4] M. Mosalanejad, S. Brebels, C. Soens, I. Ocket, and G. A. E. Vandenbosch, "Millimeter wave cavity backed microstrip antenna array for 79 GHz radar applications," *Progress In Electromagnetics Research*, vol. 158, pp. 89–98, 2017, DOI:10.2528/PIER17010407.

[5] M. I. Dessouky, H. A. Sharshar, and Y. A. Albagory, "Design of high altitude platforms cellular communications," *Progress In Electromagnetics Research*, vol. 67, pp. 251–261, 2007, DOI:10.2528/PIER06092501.

[6] M. Longhi, S. Vellucci, M. Barbuto, A. Monti, Z. Hamzavi-Zarghani, L. Stefanini, D. Ramaccia, F. Bilotti, and A. Toscano, "Array Synthesis of Circular Huygens Metasurfaces for Antenna Beam-Shaping," *IEEE Antennas and Wireless Propagation Letters*, vol. 22, no. 11, pp. 2649-2653, 2023, DOI: 10.1109/LAWP.2023.3315774.

[7] T. Isernia, O. M. Bucci, and N. Fiorentino, "Shaped beam antenna synthesis problems: Feasibility criteria and new strategies," *Journal of Electromagnetic Waves and Applications*, vol. 12, no. 1, pp. 103-138, 1998, DOI: 10.1163/156939398X00098.

[8] G. M. Battaglia, A. F. Morabito, R. Palmeri, and T. Isernia, "Constrained focusing of vector fields intensity in near zone and/or complex scenarios as a low-dimensional global optimization," *Journal of Electromagnetic Waves and Applications*, vol. 34, no. 15, pp. 1977-1989, 2020, DOI: 10.1080/09205071.2020.1801521.

[9] S. Clauzier, S. M. Mikki, and Y. M. Antar, "Design of near-field synthesis arrays through global optimization," *IEEE Transactions on Antennas and Propagation*, vol. 63, no. 1, pp. 151-165, 2014, DOI: 10.1109/TAP.2014.2367536.

[10] A. F. Morabito, A. Di Carlo, L. Di Donato, T. Isernia, and G. Sorbello, "Extending Spectral Factorization to Array Pattern Synthesis Including Sparseness, Mutual Coupling, and Mounting-Platform Effects," *IEEE Transactions on Antennas and Propagation*, vol. 67, no. 7, pp. 4548-4559, 2019, DOI: 10.1109/TAP.2019.2905977.

[11] O. M. Bucci, T. Isernia, and A. F. Morabito, "An Effective Deterministic Procedure for the Synthesis of Shaped Beams by Means of Uniform-Amplitude Linear Sparse Arrays," *IEEE Transactions on Antennas and Propagation*, vol. 61, no. 1, pp. 169–175, 2013, DOI: 10.1109/TAP.2012.2219844.

[12] A. Zhang, S. Lei, W. Yang, J. Tian, H. Hu, and L. Xiao, "Mainlobe/Sidelobe Region Gap Minimization for Shaped-Beam Pattern Synthesis via Antenna Array," *IEEE Antennas and Wireless Propagation Letters*, vol. 23, no. 1, pp. 144-148, 2024, DOI: 10.1109/LAWP.2023.3320111.

[13] O. M. Bucci, T. Isernia, and A. F. Morabito, "Optimal synthesis of circularly symmetric shaped beams," *IEEE Transactions on Antennas and Propagation*, vol. 62, no. 4, pp. 1954-1964, 2014, DOI: 10.1109/TAP.2014.2302842.

[14] A. F. Morabito, A. R. Laganà, and T. Isernia, "On the optimal synthesis of ring symmetric shaped patterns by means of uniformly spaced planar arrays," *Progress In Electromagnetics Research B*, vol. 20, pp. 33-48, 2010, DOI: 10.2528/PIERB10011206.

[15] D. Silverstein and Y. Leviatan, "Design of Irregular Embedded Antenna Arrays for Shaped-Beam Radiation Using Reciprocity and Sparse Optimization," *IEEE Transactions on Antennas and Propagation*, vol. 71, no. 4, pp. 3273-3281, 2023, DOI: 10.1109/TAP.2023.3240597.

[16] S. Zeng, X. Yang, C. Li, and F. Zhao, "Fast Descent Search Algorithm for Shaped-Beam Synthesis With the Desired Field Phases as Design Variables," *IEEE Transactions on Antennas and Propagation*, vol. 71, no. 4, pp. 3070-3079, 2023, DOI: 10.1109/TAP.2023.3243777.

[17] A. F. Vaquero, M. R. Pino, and M. Arrebola, "Adaptive Field-to-Mask Procedure for the Synthesis of Metalens Antennas With Complex Near-Field Coverage Patterns in 5G Scenarios," *IEEE Transactions on Antennas and Propagation*, vol. 71, no. 9, pp. 7158-7171, 2023, DOI: 10.1109/TAP.2023.3291431.

[18] F. Lisi, A. Michel, and P. Nepa, "Synthesis of Near-Field Arrays Based on Electromagnetic Inner Products," *IEEE Transactions on Antennas and Propagation*, vol. 71, no. 6, pp. 4919-4931, 2023, DOI: 10.1109/TAP.2023.3247892.

[19] L. W. Mou, Y. J. Cheng, Y. F. Wu, M. H. Zhao, and H. N. Yang, "Design for Array-Fed Beam-Scanning Reflector Antennas With Maximum Radiated Power Efficiency Based on Near-Field Pattern Synthesis by Support Vector Machine," *IEEE Transactions on Antennas and Propagation*, vol. 70, no. 7, pp. 5035-5043, 2022, DOI: 10.1109/TAP.2021.3111506.

[20] R. Ebrahimzadeh, S. E. Hosseininejad, B. Zakeri, A. Darvish, M. Khalily, and R. Tafazolli, "Ultra-Compact 60-GHz Near-Field Focusing Configuration Using SIW Slot Array Loaded by Transmission Coding Metasurface Lens," *IEEE Transactions on Antennas and Propagation*, vol. 72, no. 2, pp. 1977-1982, 2024, DOI: 10.1109/TAP.2023.3331775.

[21] S. Guo, D. Zhao, and B. -Z. Wang, "Dimension-Reduced Optimization for Uniform Near-Field Synthesis of Irregular Arrays," *IEEE Antennas and Wireless Propagation Letters*, vol. 21, no. 5, pp. 908-912, 2022, DOI: 10.1109/LAWP.2022.3151495.

[22] X. Wang, M. S. Tong, and G. -M. Yang, "Multifocus Multinull Near-Field Transmitting Focused Metasurface," *IEEE Transactions on Antennas and Propagation*, vol. 71, no. 4, pp. 3172-3182, 2023, DOI: 10.1109/TAP.2023.3240538.

[23] R. Elliott and G. Stern, "A new technique for shaped beam synthesis of equispaced arrays," *IEEE Transactions on Antennas and Propagation*, vol. 32, no. 10, pp. 1129-1133, 1984, DOI: 10.1109/TAP.1984.1143216.

[24] H. J. Orchard, R. S. Elliott, and G. J. Stern, "Optimizing the synthesis of shaped beam antenna patterns," *IEE Proceedings H - Microwaves, Antennas and Propagation*, vol. 132, no. 1, pp. 63-68, 1985, DOI: 10.1049/ip-h-2.1985.0013.

[25] R. S. Elliott, "Criticisms of the Woodward-Lawson method," *IEEE Antennas and Propagation Society Newsletter*, vol. 3, no. 3, pp. 43-43, 1988, DOI: 10.1109/MAP.1988.6079081.

[26] R. S. Elliott, "Woodward-Lawson versus Orchard: Round Three," *IEEE Antennas and Propagation Society Newsletter*, vol. 31, no. 2, pp. 55-56, 1989, DOI: 10.1109/MAP.1989.6095669.

[27] P. Lemaitre-Auger, S. Abielmona, and C. Caloz, "Generation of Bessel Beams by Two-Dimensional Antenna Arrays Using Sub-Sampled Distributions," *IEEE Transactions on Antennas and Propagation*, vol. 61, no. 4, pp. 1838-1849, 2013, DOI: 10.1109/TAP.2012.2232263.

[28] A. Capozzoli, C. Curcio, and A. Liseno, "Time-Harmonic Echo Generation," *IEEE Transactions on Antennas and Propagation*, vol. 59, no. 9, pp. 3234-3245, 2011, DOI: 10.1109/TAP.2011.2161548.

[29] Y. Liu, X. Huang, K. D. Xu, Z. Song, S. Yang, and Q. H. Liu, "Pattern Synthesis of Unequally Spaced Linear Arrays Including Mutual Coupling Using Iterative FFT via Virtual Active Element Pattern Expansion," *IEEE Transactions on Antennas and Propagation*, vol. 65, no. 8, pp. 3950-3958, 2017, DOI: 10.1109/TAP.2017.2708081.

This is the accepted version of the following article: Giada M. Battaglia, Tommaso Isernia, Roberta Palmeri, Maria A. Maisto, Raffaele Solimene, and Andrea F. Morabito, "Near-Field Synthesis of 1-D Shaped Patterns through Spectral Factorization and Minimally-Redundant Array-Like Representations," IEEE Transactions on Antennas and Propagation, DOI 10.1109/TAP.2024.3525137.

[30] B. Fuchs, "Synthesis of Sparse Arrays With Focused or Shaped Beampattern via Sequential Convex Optimizations," *IEEE Transactions on Antennas and Propagation*, vol. 60, no. 7, pp. 3499-3503, 2012, DOI: 10.1109/TAP.2012.2196951.

[31] Y. Liu, Z.-P. Nie, and Q. H. Liu, "A New Method for the Synthesis of Non-Uniform Linear Arrays with Shaped Power Patterns (Invited Paper)," *Progress In Electromagnetics Research*, vol. 107, pp. 349-363, 2010, DOI:10.2528/PIER10060912.

[32] A. Capozzoli and G. D'Elia, "Global Optimization and Antenna Synthesis and Diagnosis, Part Two: Applications to Advanced Reflector Antennas Synthesis and Diagnosis Techniques," *Progress In Electromagnetics Research*, vol. 56, pp. 233-261, 2006, DOI:10.2528/PIER05032503.

[33] T. Isernia, "Problemi di sintesi in potenza: criteri di esistenza e nuove strategie," *Proceedings of the Tenth Italian Meeting on Electromagnetics*, pp. 533-536, 1994.

[34] S. P. Wu, S. Boyd, and L. Vandenberghe, "FIR filter design via semidefinite programming and spectral factorization," *Proceedings of 35th IEEE Conference on Decision and Control*, vol. 1, pp. 271-276, 1996, DOI: 10.1109/CDC.1996.574313.

[35] S. P. Wu, S. Boyd, and L. Vandenberghe, "FIR Filter Design via Spectral Factorization and Convex Optimization," *Applied and Computational Control, Signals, and Circuits,* vol. 1*,* pp. 215-245, 1999, DOI: 10.1007/978-1-4612-0571-5_5.

[36] A. L. Cauchy, *Cours d'analyse de l'École Royale Polytechnique*, Chapter 10, pp. 309-347, Cambridge University Press, ISBN: 9781108002080, first published 1821 (digitally printed version 2009).

[37] O. M. Bucci, T. Isernia, A. F. Morabito, S. Perna, and D. Pinchera, "Density and element-size tapering for the design of arrays with a reduced number of control points and high efficiency," *Proceedings of the Fourth European Conference on Antennas and Propagation (EUCAP)*, pp. 1-4, 2010, DOI: https://ieeexplore.ieee.org/document/5505377.

[38] N. Decarli and D. Dardari, "Communication modes with large intelligent surfaces in the near field," *IEEE Access*, vol. 9, pp. 165648-165666, 2021, DOI: 10.1109/ACCESS.2021.3133707.

[39] D. Dardari, N. Decarli, A. Guerra, and F. Guidi, "LOS/NLOS near-field localization with a large reconfigurable intelligent surface," *IEEE Transactions on Wireless Communications*, vol. 21*,* no. 6, pp. 4282-4294, 2021, DOI: 10.1109/TWC.2021.3128415.

[40] Y. Jiang, F. Gao, M. Jian, S. Zhang, and W. Zhang, "Reconfigurable intelligent surface for near field communications: Beamforming and sensing," *IEEE Transactions on Wireless Communications*, vol. 22, no. 5, pp. 3447-3459, 2023, DOI: 10.1109/TWC.2022.3218531.

[41] Z. Wang, X. Mu, and Y. Liu, "Near-field integrated sensing and communications," *IEEE Communications Letters*, vol. 27*,* no. 8, pp. 2048-2052, 2023, DOI: 10.1109/LCOMM.2023.3280132.

[42] H. Chen, M. F. Keskin, A. Sakhnini, N. Decarli, S. Pollin, D. Dardari, and H. Wymeersch, "6G Localization and Sensing in the Near Field: Features, Opportunities, and Challenges," *IEEE Wireless Communications*, vol. 31, no. 4, pp. 260-267, 2024, DOI: 10.1109/MWC.011.2300359.

[43] V. R. Gowda, O. Yurduseven, G. Lipworth, T. Zupan, M. S. Reynolds, and D. R. Smith, "Wireless power transfer in the radiative near field," *IEEE Antennas and Wireless Propagation Letters*, vol. 15, pp. 1865-1868, 2016, DOI: 10.1109/LAWP.2016.2542138.

[44] S. R. Khan, S. K. Pavuluri, and M. P. Desmulliez, "Accurate modeling of coil inductance for near-field wireless power transfer," *IEEE Transactions on Microwave Theory and Techniques*, vol. 66, no. 9, pp. 4158-4169, 2018, DOI: 10.1109/TMTT.2018.2854190.

[45] R. G. Ayestarán, G. León, M. R. Pino, and P. Nepa, "Wireless power transfer through simultaneous near-field focusing and far-field synthesis," *IEEE Transactions on Antennas and Propagation*, vol. 67, no. 8, pp. 5623-5633, 2019, DOI: 10.1109/TAP.2019.2916677.

[46] H. Zhang, N. Shlezinger, F. Guidi, D. Dardari, M. F. Imani, and Y. C. Eldar, "Near-field wireless power transfer for 6G internet of everything mobile networks: Opportunities and challenges," *IEEE communications magazine*, vol. 60, no. 3, pp. 12-18, 2022, DOI: 10.1109/MCOM.001.2100702.

[47] P. Nepa and A. Buffi, "Near-Field-Focused Microwave Antennas: Near-field shaping and implementation," *IEEE Antennas and Propagation Magazine*, vol. 59, no. 3, pp. 42-53, 2017, DOI: 10.1109/MAP.2017.2686118.

[48] S. Loredo, G. León, and E. G. Plaza, "A Fast Approach to Near-Field Synthesis of Transmitarrays," *IEEE Antennas and Wireless Propagation Letters*, vol. 20, no. 5, pp. 648-652, 2021, DOI: 10.1109/LAWP.2021.3058847.

[49] Z. X. Huang, Y. J. Cheng, and H. N. Yang, "Synthesis of Sparse Near-Field Focusing Antenna Arrays With Accurate Control of Focal Distance by Reweighted l1 Norm Optimization," *IEEE Transactions on Antennas and Propagation*, vol. 69, no. 5, pp. 3010-3014, 2021, DOI: 10.1109/TAP.2020.3025242.

[50] R. Martin, "Approximation of Ω−bandlimited Functions by Ω−bandlimited Trigonometric Polynomials," *Sampling Theory In Signal And Image Processing,* vol. 6, no. 3, pp. 273-296, 2007, DOI: 10.1007/BF03549477.

[51] M. A Maisto, R. Pierri, and R, Solimene, "Near-Field Transverse Resolution in Planar Source Reconstructions," *IEEE Transactions on Antennas and Propagation*, vol. 69, no. 8, pp. 4836-4845, 2021, DOI: 10.1109/TAP.2021.3060030.

[52] O. M. Bucci and M. D'Urso, "Power pattern synthesis of given sources exploiting array methods," *Proceedings of the Second European Conference on Antennas and Propagation (EuCAP)*, pp. 1-6, 2007, DOI: 10.1049/ic.2007.1267.

[53] M. A. Maisto, G. Leone, A. Brancaccio, and R. Solimene, "Efficient Planar Near-Field Measurements for Radiation Pattern Evaluation by a Warping Strategy," *IEEE Access*, vol. 9, pp. 62255-62265, 2021, DOI: 10.1109/ACCESS.2021.3074786.

[54] R. Solimene, M. A. Maisto, and R. Pierri, "Sampling approach for singular system computation of a radiation operator," *Journal of the Optical Society of America A*, vol. 36, no. 3, pp. 353-361, 2019, DOI: 10.1364/JOSAA.36.000353.

[55] A. Capozzoli, C. Curcio, and A. Liseno, "Different Metrics for Singular Value Optimization in Near-Field Antenna Characterization," *Sensors*, vol. 21, no. 6, p. 2122, 2021, DOI: https://doi.org/10.3390/s21062122.

[56] A. Capozzoli, C. Curcio, A. Liseno, and P. Vinetti, "Field sampling and field reconstruction: A new perspective," *Radio Science*, vol. 45, no. 6, pp. 1-31, 2010, DOI: 10.1029/2009RS004298.

[57] T. Isernia, G. Leone, and R. Pierri, "Phase retrieval of radiated fields," *Inverse Problems*, vol. 11, no. 1, pp. 183-203, 1995, DOI: 10.1088/0266-5611/11/1/010.

[58] G. M. Battaglia, M. A. Maisto, T. Isernia, R. Palmeri, R. Solimene, and A. F. Morabito, "Extending Spectral Factorization to the Near-Field Synthesis of Shaped Beams," *4th URSI Atlantic Radio Science Meeting (AT-RASC)*, pp. 1-4, 2024, DOI:10.46620/URSIATRASC24/YJMU4127.

[59] D. Slepian, "On bandwidth," *Proceedings of the IEEE*, vol. 64, no. 3, pp. 292-300, 1976, DOI: 10.1109/PROC.1976.10110.

[60] M. A. Maisto, R. Pierri, and R. Solimene, "Near-Field Warping Sampling Scheme for Broad-Side Antenna Characterization," *Electronics,* vol. 9, no. 6, p. 1047, 2020, DOI: https://doi.org/10.3390/electronics9061047.

[61] A. Hussen and A. Zeyani, "Fejer-Riesz Theorem and Its Generalization," *International Journal of Scientific and Research Publications*, vol. 11, no. 6, pp. 286-292, 2021, DOI: 10.29322/IJSRP.11.06.2021.p11437.

[62] M. A. Maisto, R. Solimene, and R. Pierri, "Resolution limits in inverse source problem for strip currents not in Fresnel zone," *Journal of the Optical Society of America A*, vol. 36, no. 5, pp 826-833, 2019, DOI:10.1364/JOSAA.36.00082.

[63] M. A. Maisto, R. Solimene, and R. Pierri, "Valid angle criterion and radiation pattern estimation via singular value decomposition for planar scanning," *IET Microwaves, Antennas & Propagation*, vol. 13, no. 13, pp. 2342-2348, 2019, DOI: 10.1049/iet-map.2018.5240.

This is the accepted version of the following article: Giada M. Battaglia, Tommaso Isernia, Roberta Palmeri, Maria A. Maisto, Raffaele Solimene, and Andrea F. Morabito, "Near-Field Synthesis of 1-D Shaped Patterns through Spectral Factorization and Minimally-Redundant Array-Like Representations," IEEE Transactions on Antennas and Propagation, DOI 10.1109/TAP.2024.3525137.

[64] D. Slepian and H. O. Pollak, "Prolate spheroidal wave functions, Fourier analysis and uncertainty-I," *The Bell System Technical Journal*, vol. 40, pp. 43–64, 1961, DOI: 10.1002/j.1538-7305.1961.tb03976.x.

[65] R. E. Hodges and Y. Rahmat-Samii, "On sampling continuous aperture distributions for discrete planar arrays," *IEEE Transactions on Antennas and Propagation*, vol. 44, no. 11, pp. 1499-1508, 1996, DOI: 10.1109/8.542075.

[66] R. Elliott, "On discretizing continuous aperture distributions," *IEEE Transactions on Antennas and Propagation*, vol. 25, no. 5, pp. 617-621, 1977, DOI: 10.1109/TAP.1977.1141658.

[67] M. I. Skolnik, Chapter 6 "Nonuniform Arrays" in *R. E. Collin and. F.Zucker (eds) Antenna Theory*, New York, McGraw-Hill, 1969.

[68] G. M. Battaglia, A. F. Morabito, R. Palmeri, R. Abdullin, and T. Isernia, "A New Approach to the 2-D Power Synthesis of Shaped Beams with Arbitrary Footprints," *IEEE Conference on Antenna Measurements and Applications (CAMA)*, pp. 977-979, 2023, DOI: 10.1109/CAMA57522.2023.10352665.

[69] G. M. Battaglia, A. F. Morabito, R. Palmeri, and T. Isernia, "Extending Spectral Factorization to the 2-D Mask-Constrained Power Synthesis of Shaped Beams with Arbitrary Footprints," *18th European Conference on Antennas and Propagation (EuCAP)*, pp. 1-3, 2024, DOI: 10.23919/EuCAP60739.2024.10501098.

This is the accepted version of the following article: Giada M. Battaglia, Tommaso Isernia, Roberta Palmeri, Maria A. Maisto, Raffaele Solimene, and Andrea F. Morabito, "Near-Field Synthesis of 1-D Shaped Patterns through Spectral Factorization and Minimally-Redundant Array-Like Representations," IEEE Transactions on Antennas and Propagation, DOI 10.1109/TAP.2024.3525137.